PHYSICAL REVIEW A VOLUME 24, NUMBER 4 OCTOBER 1981

Unified approach to multiphoton lasers and multiphoton bistability

Margaret Reid
Physics Department, University of Auckland, Auckland, New Zealand

Kenneth J. McNeil
Physics Department, University of Waikato, Hamilton, New Zealand

Daniel F. Walls*
Joint Institute for Laboratory Astrophysics, National Bureau of Standards and University of Colorado, Boulder, Colorado 80309
(Received 9 February 1981)

This paper presents a unified theory of nonequilibrium transitions which occur in radiation interacting via an n-photon transition with atomic systems inside optical cavities. Incoherent pumping of the atoms and coherent driving of the cavity are included. Examples of such systems are the n-photon laser, the n-photon laser with injected signal, and n-photon optical bistability. The state equation and stability conditions for these phenomena are derived. Fluctuations are included via a Fokker-Planck equation in the constant-diffusion approximaton for which potential solutions may be obtained in the steady state. When these solutions are used, moments of the photon distribution can be calculated for the above systems in the specific cases of one- and two-photon transitions.

I. INTRODUCTION

We wish to present a unified treatment of n-photon transitions which can occur in an optical cavity filled with two-level atoms. These atoms are assumed to interact with only a single-cavity mode, which has no spatial variation. Our analysis thus describes interactions in a high-Q ring cavity. The cavity may be coherently driven by an external field, and the atoms may also be pumped incoherently. The evolution of the atomic and light field variables is then described by the Maxwell-Bloch equations with appropriate terms for losses and external pumping. In a high-Q cavity the atomic variables relax more rapidly than the field variables, and can be eliminated adiabatically from the Maxwell-Bloch equations, resulting in an equation of motion for the cavity-field mode only. The aim of this paper is to show how a number of different systems may be treated using the same formalism, and indeed, arise as different limits of this single equation. This equation contains parameters representing the external driving field and the atomic pumping, and for the appropriate values of these parameters, the equation describes the n-photon laser, the n-photon laser with injected field, or n-photon optical bistability.

Fluctuations are considered in a phenomenological fashion by adding a thermal-type Langevin force to the equation for the light field. This random force will represent thermal noise in the light due, for example, to spontaneous emission of the atoms in lasing systems or to any thermal noise component present in the driving field. In general, quantum fluctuation terms, which depend on the field variable should also be included, but we shall assume that such terms are negligible compared to the thermal noise term. In this paper we shall study the Fokker-Planck equation corresponding to this Langevin equation, and obtain the steady-state probability distribution for the field amplitude in potential-solution form. Moments of this distribution such as the mean intensity and variance of intensity fluctuations may be calculated exactly. Furthermore, the potential may be used to investigate the stability of solutions in regions where the distribution is multipeaked and the deterministic equations have multiple steady states.

II. GENERAL FORMULATION: THE n-PHOTON TRANSITION

We shall consider an optical cavity filled with a medium consisting of N two-level atoms that interact with a resonant cavity-field mode, whose spatial variation is neglected. The n-photon interaction with the atoms can be represented by an effective Hamiltonian where a summation over intermediate states is implicit, and atomic and field mode damping can be represented by interaction with reservoirs. The full Hamiltonian, in the electric dipole and rotating wave approximations, is then

$$H=\sum_{j=1}^{5} H_j ,$$

$$H_1=\hbar\omega_0 a^\dagger a+\tfrac{1}{2}n\hbar\omega_0\sum_{\mu=1}^{N}\sigma_\mu^z ,$$

$$H_2=i\hbar\sum_{\mu=1}^{N}[\,ge^{-i\vec{k}\cdot\vec{r}_\mu}(a^\dagger)^n\sigma_\mu^- - ge^{i\vec{k}\cdot\vec{r}_\mu}a^n\sigma_\mu^+\,], \quad (2.1)$$

$$H_3=\sum_{\mu=1}^{N}(\sigma_\mu^+\Gamma_A+\sigma_\mu^-\Gamma_A^\dagger),$$

$$H_4=a^\dagger\Gamma_F+a\Gamma_F^\dagger,$$

$$H_5=i\hbar(a^\dagger\mathcal{E}e^{-i\omega_0 t}-a\mathcal{E}^*e^{i\omega_0 t}).$$

Here, a, $a^\dagger$ are the boson operators for the field mode and $\sigma^\pm$, σ^z are the Pauli atomic operator for the μth atom. ω_0 is the cavity resonance frequency, with $n\omega_0$ taken to be equal to the atomic resonance frequency. The coherent external driving field is taken to have the same frequency ω_0, and its amplitude is $\mathcal{E}$. Γ_A, $\Gamma_A^\dagger$ represent the reservoir for the atoms, describing both incoherent pumping and radiative damping; Γ_F, $\Gamma_F^\dagger$ represent the reservoir describing damping of the cavity mode. g is the n-photon matrix element for the coupling between the field mode and the atoms. We note here that because we have taken the field to be in exact resonance for the n-photon atomic transition, our analysis corresponds to the purely absorptive situation. In the case of one-photon transitions in this system, a more general analysis allowing for off-resonance situations has recently been given by Graham and Schenzle.[1]

The system can be described by the cavity mode operator a, the total atomic polarization $J^+=\sum_{\mu=1}^{N}\sigma_\mu^+e^{i\mathbf{k}\cdot\mathbf{r}_\mu}$, and the total atomic inversion $J^z=\frac{1}{2}\sum_{\mu=1}^{N}\sigma_\mu^z$. The problem may be analyzed fully quantum mechanically using master equation and Fokker-Planck techniques as described by Haken,[2] Lax,[3] and Mandel.[4] In this paper we shall not attempt this, but rather, we shall use a semiclassical approach with the classical variables $\alpha=\langle a\rangle$, $\alpha^*=\langle a^\dagger\rangle$, $v^*=\langle J^-\rangle$, $v=\langle J^+\rangle$, and $D=\langle J_z\rangle$. Then, in the limit of zero fluctuations, when all correlation functions are assumed to factorize, the system is described by the following Maxwell-Bloch equations:

$$\begin{aligned}\dot v&=-\gamma_\perp v+2g\alpha^nD,\\ \dot D&=-\gamma_\parallel(D-D_0)-g[(\alpha^*)^nv+\alpha^nv^*],\\ \dot\alpha&=-\kappa(\alpha-E)+ngv(\alpha^*)^{n-1}.\end{aligned}\tag{2.2}$$

$\gamma_\perp$ and $\gamma_\parallel$ are the damping rates for the atomic polarization and inversion, respectively, and κ is the damping rate for the cavity field. $E=\mathcal{E}/\kappa$ is proportional to the driving field amplitude. D_0 is the inversion that would result due to the incoherent pumping of the atoms in the absence of any interaction with the field.

By appropriate choice of the external driving E and incoherent pumping these equations describe the following situations: (i) the n-photon laser: $E=0$, $D_0>0$ ($D_0=N/2$ for complete inversion); (ii) the n-photon laser with injected signal: $E\neq0$, $D_0>0$; (iii) n-photon optical bistability: $E\neq0$, $D_0<0$.

A. Adiabatic elimination of the atomic variables; the steady-state solutions

In the high-Q-cavity limit, we have $\kappa\ll\gamma_\perp,\gamma_\parallel$ and the atomic variables may be adiabatically eliminated, that is, replaced by the values obtained by setting $\dot v$ and $\dot D$ equal to zero in Eqs. (2.2):

$$\begin{aligned}D&=D_0\left[1+\left(\frac{|\alpha|^2}{n_0}\right)^n\right]^{-1},\\ v&=2g\frac{D_0}{\gamma_\perp}\left[1+\left(\frac{|\alpha|^2}{n_0}\right)^n\right]^{-1}\alpha^n,\end{aligned}\tag{2.3}$$

where

$$n_0=\left(\frac{\gamma_\parallel\gamma_\perp}{4g^2}\right)^{1/n}.$$

Substitution of these expressions in the equation for α in Eqs. (2.2) gives the following equation for the field mode alone:

$$\frac{\partial\alpha}{\partial\tau}=-(\alpha-E)-2nC\left[1+\left(\frac{|\alpha|^2}{n_0}\right)^n\right]^{-1}|\alpha|^{2(n-1)}\alpha,\tag{2.4}$$

where $\tau=\kappa t$ and $C=g^2(-D_0)/\kappa\gamma_\perp$. The steady-state version of this equation can be written in the following scaled form:

$$y=x\left(1+\frac{C_n|x|^{2(n-1)}}{1+|x|^{2n}}\right),\tag{2.5}$$

where

$$x=\left(\frac{4g^2}{\gamma_\parallel\gamma_\perp}\right)^{1/2n}\alpha,\quad y=\left(\frac{4g^2}{\gamma_\parallel\gamma_\perp}\right)^{1/2n}E,$$

and

$$C_n=2nC(n_0)^{n-1}.$$

B. Stability of the steady states

For certain values of E and D_0, Eq. (2.5) yields multiple solutions, and it becomes necessary to determine the stability of such solutions. If Eq. (2.4) is written $\dot\alpha=F(\alpha,\alpha^*)$, standard linearization procedure gives the following linear equation for small perturbations $\delta\alpha$, $\delta\alpha^*$ about the steady-state values α_0, α_0^*:

$$\frac{\partial}{\partial\tau}\begin{bmatrix}\delta\alpha\\ \delta\alpha^*\end{bmatrix}=\begin{bmatrix}\frac{\partial F}{\partial\alpha}(\alpha_0,\alpha_0^*) & \frac{\partial F}{\partial\alpha^*}(\alpha_0,\alpha_0^*)\\ \frac{\partial F^*}{\partial\alpha}(\alpha_0,\alpha_0^*) & \frac{\partial F^*}{\partial\alpha^*}(\alpha_0,\alpha_0^*)\end{bmatrix}\begin{bmatrix}\delta\alpha\\ \delta\alpha^*\end{bmatrix}.\tag{2.6}$$

The condition for stability that the real parts of

the eigenvalues of the matrix (called A for convenience) in Eq. (2.6) be negative requires $\mathrm{Tr}(A) < 0$ and $\mathrm{Det}(A) > 0$, i.e.,

$$\frac{\partial\,\mathrm{Re}F}{\partial u}+\frac{\partial\,\mathrm{Im}F}{\partial v}<0\,,$$
$$\frac{\partial\,\mathrm{Re}F}{\partial u}\frac{\partial\,\mathrm{Im}F}{\partial v}-\frac{\partial\,\mathrm{Re}F}{\partial v}\frac{\partial\,\mathrm{Im}F}{\partial u}>0\,, \tag{2.7}$$

where $u=\mathrm{Re}(\alpha)$, $v=\mathrm{Im}(\alpha)$. Equation (2.4) may be written $\dot{\alpha}=\kappa E-\alpha f(I)$, where $I=|\alpha|^2$ and f is real, in which case the stability conditions (2.7) become

$$f(I)+I\frac{df(I)}{dI}>0\,,$$
$$f(I)\left(f(I)+2I\frac{df(I)}{dI}\right)>0\,, \tag{2.8}$$

where f is evaluated at the steady-state value for I. In the following sections we will be considering photon distributions in terms of a potential, so it is convenient here to use the stability conditions (2.7) to introduce a potential $\phi(u,v)$ by defining

$$\frac{\partial\phi(u,v)}{\partial u}=-\,\mathrm{Re}F(u,v)\,,$$
$$\frac{\partial\phi(u,v)}{\partial v}=-\,\mathrm{Im}F(u,v)\,. \tag{2.9}$$

The steady-state solutions of Eq. (2.4) thus correspond to the turning points of $\phi(u,v)$. In terms of $\phi(u,v)$ the stability conditions (2.7) become

$$\frac{\partial^2\phi}{\partial u^2}+\frac{\partial^2\phi}{\partial v^2}>0\,,$$
$$\left(\frac{\partial^2\phi}{\partial u^2}\right)\left(\frac{\partial^2\phi}{\partial v^2}\right)-\left(\frac{\partial^2\phi}{\partial u\partial v}\right)^2>0\,, \tag{2.10}$$

which show that only those solutions of Eq. (2.4) which correspond to a local minimum of $\phi(u,v)$ are stable. We shall examine the stability of solutions for each of the physical situations discussed in the following sections.

C. Fluctuations

We shall introduce fluctuations in a phenomenological manner by simply adding a δ-correlated fluctuating force to the equation of motion for α [Eq. (2.4)], and treat α as a stochastic variable:

$$\frac{\partial\alpha}{\partial\tau}=-(\alpha-E)-2nC\left[1+\left(\frac{|\alpha|^2}{n_0}\right)^n\right]^{-1}|\alpha|^{2(n-1)}\alpha+\xi(t)\,, \tag{2.11}$$

with $\langle\xi(t')\xi^*(t)\rangle=\Lambda\delta(t-t')$ and $\langle\xi(t)\xi(t')\rangle=0$. In this paper we shall use the Fokker-Planck equation equivalent to Eq. (2.10), and consider the probability distribution $P(\alpha,\alpha^*,\tau)$ for α:

$$\frac{\partial P(\alpha,\alpha^*,\tau)}{\partial\tau}=-\frac{\partial}{\partial\alpha}\left\{-(\alpha-E)-2nC\left[1+\left(\frac{|\alpha|^2}{n_0}\right)^n\right]^{-1}|\alpha|^{2(n-1)}\alpha\right\}P$$
$$-\frac{\partial}{\partial\alpha^*}\left\{-(\alpha^*-E^*)-2nC\left[1+\left(\frac{|\alpha|^2}{n_0}\right)^n\right]^{-1}|\alpha|^{2(n-1)}\alpha\right\}P+2\bar{n}\frac{\partial^2P}{\partial\alpha\partial\alpha^*}\,. \tag{2.12}$$

$\bar{n}=\Lambda/2\kappa$ represents thermal noise which may arise from spontaneous emission by the atoms or fluctuations in the driving field. As mentioned in the introduction a full analysis shows the existence of nonthermal-type noise, which is a function of α, and which we call "quantum noise." Hence, our analysis applies to the situation where thermal-type noise is the dominant noise. In the case of the laser, the noise due to spontaneous emission of the atom consists of a leading constant term, followed by terms which are functions of α, and standard treatments retain only the constant term.[5] Comparison with exact results has shown that this is a very good approximation.[4] In the case of optical bistability, however, the fully quantum-mechanical Fokker-Planck equation has a noise function in which the leading term is not a constant.[6,7] Thus Eq. (2.12) will very adequately describe lasers with $\bar{n}$ representing noise due to spontaneous emission. For optical bistability, Eq. (2.12) will give an adequate description only when the thermal noise $\bar{n}$ dominates the quantum noise.

D. Steady-state solutions of the Fokker-Planck equation

Equation (2.12) can be readily shown to obey potential conditions[8] and has the steady-state solution

$$P(\alpha,\alpha^*)=Ne^{-\phi(\alpha,\alpha^*)}\,, \tag{2.13}$$

where N is a normalization constant, and the potential $\phi(\alpha,\alpha^*)$ is given by

$$\phi(\alpha,\alpha^*)=\frac{1}{n}(|\alpha|^2-E^*\alpha-E\alpha^*)$$
$$-H\ln\left[1+\left(\frac{|\alpha|^2}{n_0}\right)^n\right], \tag{2.14}$$

where

$$H=\gamma_{\parallel}D_0/\Lambda\,.$$

This is a general result, and by suitable choices of the parameters, E and D_0 give the photon statistics of n-photon lasers with or without an injected signal and n-photon bistability. We shall consider these systems in more detail for the special cases of one- and two-photon transitions in the following two sections.

III. ONE-PHOTON TRANSITIONS

A. The laser

1. Semiclassical analysis

The semiclassical equation for the usual one-photon laser[9] is obtained from Eq. (2.4) by setting $E=0$ (no external driving field) and taking D_0 positive (representing external incoherent pumping of the atoms). The steady-state equation (2.5) in scaled form is thus

$$x\left(1-\frac{C_1}{1+|x|^2}\right)=0\,, \tag{3.1}$$

where $C_1=2g^2D_0/\kappa\gamma_\perp$ is redefined to be positive. Setting $x=re^{i\theta}$, we find the solutions

$$r=\begin{cases}0\,, & C_1>0\\ (C_1-1)^{1/2}\,, & C_1>1\end{cases} \tag{3.2}$$

with θ arbitrary. The stability conditions (2.8) for this case are (in terms of the scaled intensity $I=r^2$)

$$\begin{aligned}&I^2+2I+1-C_1>0\,,\\ &(I+1-C_1)[I^2+I(C_1+2)+1-C_1]>0\,.\end{aligned} \tag{3.3}$$

The solution $r=0$ is thus stable only for $C_1<1$; $I=C_1-1$ is the only stable solution for $C_1>1$. The laser thus undergoes a far from equilibrium second-order phase transition at the threshold $C_1=1$, or $D_0=\kappa\gamma_\perp/2g^2$.[10,11]

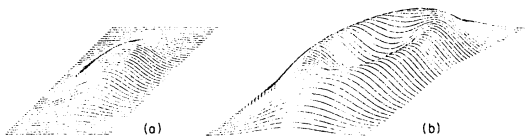

FIG. 1. Probability distribution for the one-photon laser (a) 1.1 ×threshold; (b) 3× threshold.

2. Fluctuations

A quantum theory of the laser in which a Fokker-Planck equation of the form (2.12) with a constant noise term was derived was first given by Risken.[5] A commonly used approximation is to expand the term $(1+|\alpha|^2/n_0)^{-1}$ to first order in $|\alpha|^2$, giving a driven Van der Pol oscillator type of equation. Here, we shall retain the full expression. The resulting potential (2.14) for the one-photon laser is then

$$\phi(\alpha,\alpha^*)=\frac{|\alpha|^2}{\bar{n}}-H\ln\left(1+\frac{|\alpha|^2}{n_0}\right). \tag{3.4}$$

The corresponding probability distribution $P=\mathrm{Ne}^{-\phi}$ is shown in Fig. 1 for various values of D_0.

As discussed in Sec. II, the maxima and minima of the potential ϕ [which is proportional to $-\log P(\alpha,\alpha^*)$] correspond to the unstable and stable solutions, respectively, of the semiclassical equations. Below threshold the potential is a steeply sloped well with a minimum at $r=0$, and fluctuations away from this minimum are quickly damped. As D_0 approaches its threshold value, the potential becomes shallower, and fluctuations away from $r=0$ take an increasingly longer time to decay. This is the well-known phenomenon of critical slowing down. Above threshold the origin $r=0$ becomes a maximum corresponding to the semiclassical solution, $r=0$ becoming unstable and the potential has its minimum on the circle $r=(C_1-1)^{1/2}$ corresponding to the stable semiclassical solution.

3. Photon statistics

The steady-state moments may be calculated using the solution given by Eqs. (2.13) and (2.14), with $n=1$. The unnormalized intensity moments $I^{(i)}$ are

$$\begin{aligned}I^{(i)}&=\int d^2\alpha\,|\alpha|^{2i}P(\alpha,\alpha^*)\\ &=\int_0^\infty dR\left(1+\frac{R}{n_0}\right)^H R^i e^{-R/\bar{n}}\int_0^{2\pi}d\theta\exp\left(2E_0\sqrt{R}\,\frac{\cos(\theta-\theta_0)}{\bar{n}}\right).\end{aligned} \tag{3.5}$$

Here we have set $\alpha=\sqrt{R}\,e^{i\theta}$ and $E=E_0e^{i\theta_0}$. The driving field E has been retained so that this general result can be used in the following sections on the laser with injected signal and optical bistability. The θ integral in Eq. (3.5) is the integral representation of the Bessel function $I_0(2E_0\sqrt{R}/\bar{n})$.[12] Expanding I_0 in a power series and carrying out the integration over R term by term we find

$$I^{(i)}=\pi n_0^{i+1}\sum_{k=0}^{\infty}\frac{[(E_0/\bar{n})\sqrt{n_0}]^{2k}}{(k!)^2}(k+i)!\,U\left(k+i+1,k+H+i+2;\frac{n_0}{\bar{n}}\right), \tag{3.6}$$

where Γ is the gamma function and U is the second confluent hypergeometric function.[12] Equation (3.6) is a general expression for the unnormalized intensity moments of one-photon transitions with arbitrary inversion D_0 and coherent driving field E_0. The normalized intensity moments are

$$\langle a^{\dagger i} a^i \rangle = I^{(i)}/I^{(0)} . \tag{3.7}$$

For the laser, $E_0 = 0$, and we obtain the following expression for the mean $\langle n \rangle = \langle a^\dagger a \rangle$:

$$\langle n \rangle = n_0 \frac{U(2, H+3; n_0/\bar{n})}{U(1, H+2; n_0/\bar{n})} . \tag{3.8}$$

The normalized second-order correlation function $g^{(2)}(0) = \langle a^{\dagger 2} a^2 \rangle / \langle a^\dagger a \rangle^2$ is

$$g^{(2)}(0) = 2 \frac{U(3, H+4; n_0/\bar{n}) U(1, H+2; n_0/\bar{n})}{[U(2, H+3, n_0/\bar{n})]^2} . \tag{3.9}$$

These expressions for $\langle n \rangle$ and $g^{(2)}(0)$, together with the semiclassical mean intensity given by Eq. (3.2), are plotted as functions of the incoherent atomic pumping D_0 in Fig. 2. Below the threshold $C_1 = 1$, we have $g^{(2)}(0) = 2$, characteristic of chaotic or thermal light. In this region the light field is generated by spontaneous emission of the atoms. Above threshold the atoms begin emitting coherently and $g^{(2)}(0) \to 1$, characteristic of coherent light. One finds that the smaller the noise, $\bar{n}$, the sharper the transition from $g^{(2)}(0) \simeq 2$ to $g^{(2)}(0) \simeq 1$.

The photon number distribution P_n may be readily calculated from $P(\alpha, \alpha^*)$. The P_n are the diagonal elements of the light field-density operator in the number (or Fock) state representation, and we have

$$P_n = \int d^2\alpha \, |\langle n | \alpha \rangle|^2 P(\alpha, \alpha^*)$$

$$= n_0^{n+1} U\left(n+1, H+n+2; \frac{n_0}{\bar{n}} + n_0\right) . \tag{3.10}$$

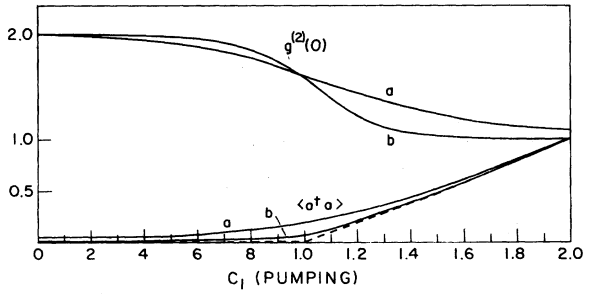

FIG. 2. Moments of the one-photon laser. Mean intensity $\langle a^\dagger a \rangle$ and second-order correlation function $g^{(2)}(0)$ for (a) $n_0/\bar{n} = 20$; (b) $n_0/\bar{n} = 100$; semiclassical mean ----.

Note that P_n here are not normalized; normalization is carried out by requiring $\sum_{n=0}^{\infty} P_n = 1$. Photon number distributions of this form have been derived from a master equation by Scully and Lamb[13] and from a Fokker-Planck equation by Lax and Louisell[14] and were first verified experimentally by Arecchi *et al.*[15]

Well below threshold the distribution becomes the Bose-Einstein power law distribution of chaotic light, and well above threshold it tends to the Poisson distribution of coherent light.

B. Laser with injected signal

We now allow an external coherent field to be injected into the laser cavity. We may use the analysis of the preceding section, with E_0 the driving field, nonzero.

1. Semiclassical results

The steady-state equation in scaled form [Eq. (2.5)] for this situation is

$$y = x\left(1 - \frac{C_1}{1+|x|^2}\right), \tag{3.11}$$

where $C_1 = 2g^2 D_0/\kappa\gamma_\perp$ is redefined to be positive. Setting $y = y_0 e^{i\theta_0}$ and $x = re^{i\theta}$, the real and imaginary parts of Eq. (3.11) are

$$y_0 \cos\theta_0 = r\cos\theta\left(1 - \frac{C_1}{1+r^2}\right),$$
$$y_0 \sin r_0 = r\sin\theta\left(1 - \frac{C_1}{1+r^2}\right). \tag{3.12}$$

These give the in-phase solution

$$\theta = \theta_0 , \tag{3.13}$$
$$y_0 = r\left(1 - \frac{C_1}{1+r^2}\right), \quad 1 - \frac{C_1}{1+r^2} > 0$$

and the out-of-phase solution

$$\theta = \theta_0 + \pi , \tag{3.14}$$
$$y_0 = -r\left(1 - \frac{C_1}{1+r^2}\right), \quad 1 - \frac{C_1}{1+r^2} < 0 .$$

In both cases we have

$$|y|^2 = |x|^2\left(1 - \frac{C_1}{1+|x|^2}\right)^2 . \tag{3.15}$$

The state equation, given by Eqs. (3.13) and (3.14) together, is plotted in Fig. 3, which shows x as a function of y. For $C_1 < 1$, x is a single-valued function of y. For $C_1 > 1$, x becomes a multiple valued function of y, and for $y < y_m$ there are three solutions for the cavity field x. However, the stability conditions [Eq. (3.3)] show that the out-of-phase solutions x_2 and x_3 are unstable;

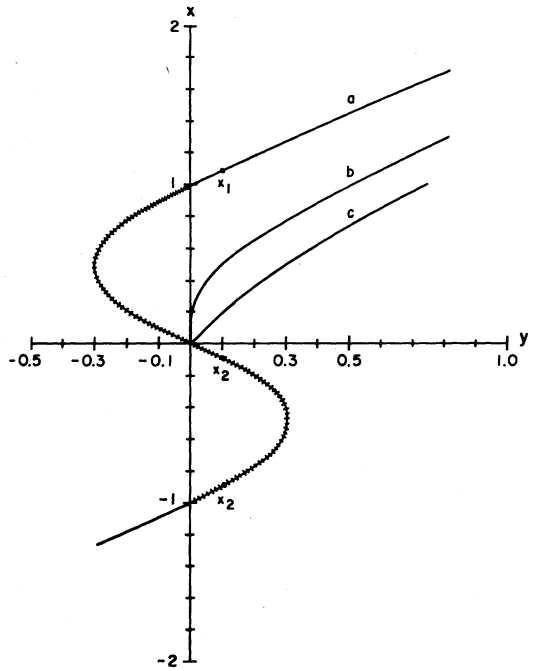

FIG. 3. One-photon laser with injected signal: output field amplitude x versus input field amplitude y. (a) $C_1=2$; (b) $C_1=1$; (c) $C_1=0.5$, —— stable, ////// unstable.

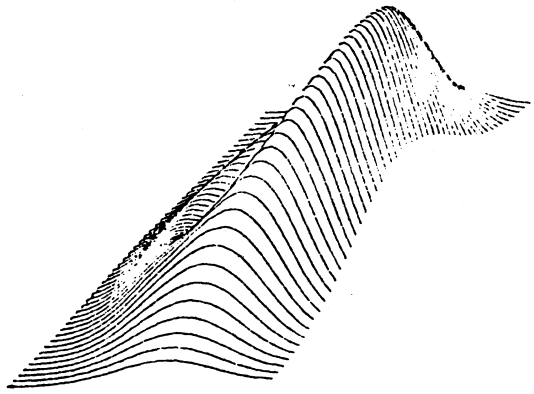

FIG. 4. Probability distribution for the one-photon laser with an injected signal ($\theta_0=0$, $E_0=0.25$, 1.6 × threshold).

only the in-phase solution x_1 is stable. Thus, although the semiclassical equations show that a multiple solution regime exists, the laser with an injected signal does not exhibit bistability, a fact noted by Lugiato[16] and by Drummond.[17] A study of the potential, in the next section, shows more clearly why in the multiple steady-state region only one solution is stable.

2. *Fluctuations*

The Fokker-Planck equation for the laser with an injected signal has a potential solution of the form of Eq. (2.12) with the potential ϕ given by Eq. (2.13), with $n=1$:

$$\phi(\alpha,\alpha^*)=\frac{1}{n}[\,|\alpha|^2-(E\alpha^*+E^*\alpha)] - H\ln\left(1+\frac{|\alpha|^2}{n_0}\right). \tag{3.16}$$

Recalling from Sec. II, that provided the noise term in the Fokker-Planck equation is independent of α, the extrema of the potential correspond to the steady-state semiclassical solutions, we examine the extrema of Eq. (3.16). Points on the upper branch of the α vs E curve (Fig. 3) correspond to minima in ϕ and are thus stable. Points on the middle branch correspond to local maxima and are therefore unstable. Points on the lower branch correspond to saddle points of the potential. A one-dimensional analysis, in which phase is ignored, gives a potential which is a planar "slice" of the two-dimensional potential. Slicing through the saddle point will then show a minimum corresponding to a point on the lower branch, leading to the wrong conclusion that the lower branch is stable. The true picture is thus given by the two-dimensional analysis which shows that since points on the lower branch correspond to saddle points in the potential, the lower branch is unstable to phase fluctuations. In Fig. 4, the distribution function $P(\alpha,\alpha^*)$ [proportional to $-\log[\phi(\alpha,\alpha^*)]$ shows clearly what is happening. With zero driving field the laser distribution is spherically symmetric, with a minimum at the origin corresponding to the maximum in the potential, surrounded by a circular ridge peaked on the circle $r=(C_1-1)^{1/2}$ corresponding to the minima in ϕ. When the external field $E=E_0e^{i\theta_0}$ is introduced, a ridge builds up along the line $\theta=\theta_0$, a valley developes along the line $\theta=\theta_0+\pi$, and the minimum at the origin moves out towards the saddle point formed where this valley cuts the original circular ridge. As E_0 is further increased, the valley along $\theta=\theta_0+\pi$ flattens out, removing the original circular ridge until E_0 is such that $y>y_m$, when only a single isolated peak along the line $\theta=\theta_0$ remains. This form of potential was first found by Chow *et al.*[18]

C. Optical bistability

1. *Semiclassical results*

Equation (2.4) may also be used to describe optical bistability, which may occur when passive atoms are placed in a coherently driven cavity. Since the atoms are not externally pumped, D_0 is now negative; in fact, $D_0=-N/2$. In the one-pho-

ton atomic transition case the scaled steady-state equation (2.5) becomes

$$y = x\left(1 + \frac{2C}{1+|x|^2}\right), \tag{3.17}$$

where $C = g^2N/2\kappa\gamma_\perp$. This equation for absorptive bistability was first derived by Bonifacio and Lugiato.[19] Experimental observation of absorptive bistability from a two-level system has recently been reported by Sandle and Gallagher.[20]

Substituting $y = y_0 e^{i\theta_0}$ and $x = re^{i\theta}$ in Eq. (3.17) we find

$$y_0 = r\left(1 + \frac{2C}{1+r^2}\right), \qquad \theta = \theta_0 . \tag{3.18}$$

The output field x is thus always in phase with the input field, and the analysis (at least when there are no fluctuations) need only be one dimensional. The analysis of the turning points of the state equation (3.18) shows that for $C < 4$ there is only one turning point and the output is a single-valued function of the input y. For $C > 4$ there are two turning points, giving a region where x is multiple valued. The linearized stability analysis shows that the upper and lower branches are stable and the middle branch is unstable, so the system is bistable in this region.

2. *Fluctuations*

If fluctuations are now included, the problem is no longer one dimensional; there will now be a distribution of phase about the most probable value θ_0. As mentioned in Sec. II, the Fokker-Planck equation for optical bistability will only be of the form [Eq. (2.12)] when the thermal noise $\bar{n}$ is much greater than the quantum noise. This thermal noise may be noise in the optical cavity and atomic medium or may also be viewed as an approximation to the noise in the applied driving field. In this high-thermal-noise limit then, the steady-state distribution is of the form given by Eqs. (2.13) and (2.14), with $D_0 = -N/2$. The potential is thus

$$\phi(\alpha, \alpha^*) = \frac{1}{\bar{n}}\left[|\alpha|^2 - E^*\alpha - E\alpha^* + \frac{\gamma_\parallel N}{2\Lambda}\ln\left(1 + \frac{|\alpha|^2}{n_0}\right)\right]. \tag{3.19}$$

This potential for absorptive bistability was first derived by Bonifacio, Gronchi, and Lugiato[21] and Schenzle and Brand.[23] The form of the steady-state distribution in the bistable region is shown in Fig. 5 (see also Ref. 22). The effect of the fluctuations is to give a probability spread about the semiclassical solutions. The unnormalized intensity moments for this distribution are given by Eq. (3.6), with $D_0 = -N/2$. We have plotted the root-mean intensity $(\langle a^\dagger a\rangle)^{1/2}$ as a function of input field in Fig. 6 together with the semiclassical result for x from Eq. (3.17). Also shown is the second-order correlation function $g^{(2)}(0)$. As expected, the root-mean intensity shows no bistability; the inclusion of fluctuations makes the upper and lower branches metastable rather than absolutely stable. In order to observe bistability (that is, hysteresis effects) the input field must be ramped in time intervals which are short compared to the lifetimes of the metastable branches. The statistics of the output light on the lower and upper branches may be deduced from $g^{(2)}(0)$. On the lower branch, $g^{(2)}(0) \simeq 2$, showing the transmission of thermal noise, whereas on the upper

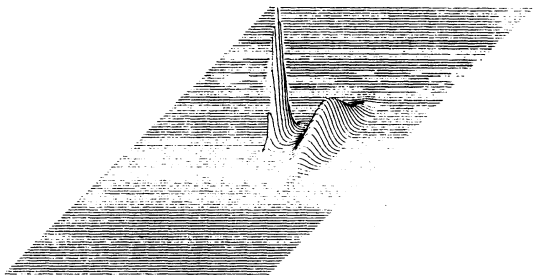

FIG. 5. Probability distribution for one-photon bistability.

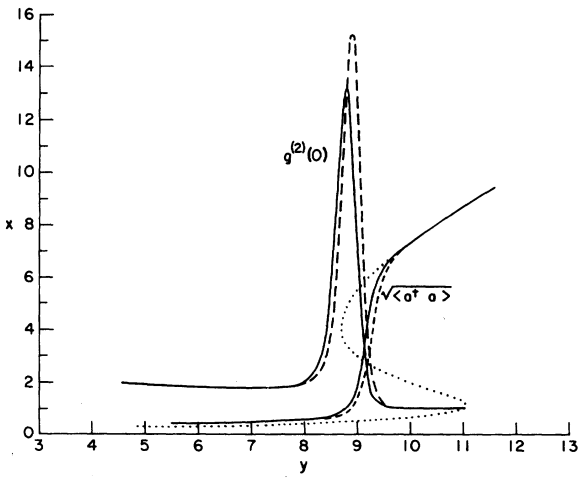

FIG. 6. Moments for one-photon bistability. Root-mean intensity $(\langle a^\dagger a\rangle)^{1/2}$ and second-order correlation function — compared to one-dimensional approximation ---, semiclassical amplitude ···. Parameters $C = 10$, $n_0 = 1$, $\bar{n} = 1$.

branch, $g^{(2)}(0) \simeq 1$, implying that the device now transmits only the coherent signal. In the threshold region there is a marked increase in $g^{(2)}(0)$, corresponding to an increase in the size of relative fluctuations. This increase in fluctuations is due to there being appreciable probabilities of the system being in either of two states, so that fluctuations between the two states will be common. For small values of the noise parameter $\bar{n}$, the probability distribution is aligned fairly narrowly along $\theta = \theta_0$, and as an approximation may be regarded as one dimensional, which was, in fact, done by Schenzle and Brand[22] in their analysis. We note that $\bar{n}$ cannot be made too small because it is assumed that thermal noise must always be much larger than the quantum noise. For comparison, we have also plotted in Fig. 6 the root-mean intensity and $g^{(2)}(0)$ obtained from Eq. (3.6), with the approximation $\theta = \theta_0$.

D. Saturable absorber with chaotic driving field

In the preceding section, the intracavity atoms are passive and thus act as a saturable absorber. The analysis used there can be used to describe systems driven by chaotic rather than coherent light. As mentioned previously, any chaotic component in the input field can be included in the noise term $\bar{n}$. If the coherent part E is zero, the above analysis then describes a system driven by entirely chaotic light. Such a system has been studied recently by Drummond *et al.*[23] whose potential solution corresponds to Eq. (3.19), with $E = 0$. In that work it was found that over a certain critical region of chaotic input intensity, the fluctuations in the output field markedly increased; that is, there was an enhanced-photon-bunching effect.

IV. TWO-PHOTON TRANSITIONS

A. The two-photon laser

A laser based on a two-photon atomic transition was first proposed by McNeil and Walls,[24] although this has not been realized in practice. Further theoretical investigations have been pursued by Gortz and Walls,[25] Ito and Nakagomi,[26] Bulsara and Schieve,[27] and Nayak and Mohanty.[28] More recently a study of n-photon lasers along lines similar to what we shall present here has been done by Sczaniecki.[29]

Two-photon transition systems will be described by the state equation (2.5) and the potential (2.14), with $n = 2$. In the case of a two-photon lasing system, there is of course no input field, so $E = 0$, and the atomic pumping D_0 is positive. The state equation (2.5) is then

$$x\left(1 - \frac{C_2|x|^2}{1+|x|^4}\right) = 0, \tag{4.1}$$

where $C_2 = (2gD_0/\kappa)(\gamma_\parallel/\gamma_\perp)^{1/2}$. The solution for the amplitude is $x = 0$ for all C_2,

$$|x|^2 = C_2/2 \pm \tfrac{1}{2}(C_2^2 - 4)^{1/2}, \quad C_2 \geq 2 \tag{4.2}$$

and the phase is arbitrary. The stability conditions [Eq. (2.8)] are

$$I^4 + 2I^2 - 2C_2 I + 1 > 0 \tag{4.3a}$$

$$(I^2 - C_2 I + 1)(I^4 + C_2 I^3 + 2I^2 - 3C_2 I + 1) > 0. \tag{4.3b}$$

It is easily seen that in contrast to the one-photon laser the $x = 0$ solution is stable for all values of the pumping parameter C_2. From Eqs. (4.3) the solution $|x|^2 = C_2/2 + \frac{1}{2}(C_2^2 - 4)^{1/2}$ is found to be stable, while the solution $|x|^2 = C_2/2 - \frac{1}{2}(C_2^2 - 4)^{1/2}$ is unstable. Thus for $C_2 > 2$ the two-photon laser is bistable. The state equation (4.2) is plotted in Fig. 7. This curve is slightly different from the usual bistability curve because the middle branch meets the lower branch only at $C_2 = \infty$. Thus, in the absence of fluctuations, as the pumping parameter C_2 is increased the system will always remain on the lower branch $x = 0$, even when $C_2 > 2$. In order to make the transition to the upper branch for $C_2 > 2$ and start lasing, fluctuations are essential.

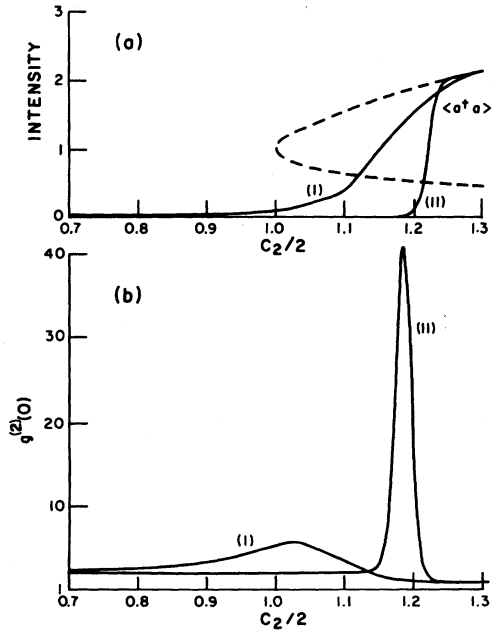

FIG. 7. Moments of the two-photon laser. (a) Mean intensity $\langle a^\dagger a \rangle$ versus atomic pumping C_2 for $n_0/\bar{n}$ equal to (I) 20, (II) 100, semiclassical intensity ---. (b) Second-order correlation functions $g^{(2)}(0)$ vs C_2 for $n_0/\bar{n}$ equal to (I) 20, (II) 100.

1. Fluctuations

Noise due to spontaneous emission of atoms, together with any thermal noise, can be taken into account by using a Fokker-Planck equation of the form of Eq. (2.12), with $n=2$ to describe the system. The potential has the form of Eq. (2.14), with $n=2$ and the driving field $E=0$:

$$\phi(\alpha,\alpha^*)=\frac{|\alpha|^2}{\bar{n}}-H\ln\left[1+\left(\frac{|\alpha|^2}{n_0}\right)^2\right]. \tag{4.4}$$

The corresponding probability distribution $P(\alpha,\alpha^*)=Ne^{-\phi(\alpha,\alpha^*)}$ is plotted in Fig. 8. Below the threshold $C_2=2$, or $D_0=(\kappa/g)(\gamma_\perp/\gamma_\parallel)^{1/2}$, the distribution is peaked at zero. Above threshold this peak remains, since the zero solution is stable even above threshold, and a new peak corresponding to the solution $|x|^2=C_2/2+\frac{1}{2}(C_2^2-4)^{1/2}$ develops. As C_2 is increased, the maximum at zero becomes smaller, and for $C_2\gtrsim 4$ it is insignificant compared to the peak at $|x|^2=C_2/2+\frac{1}{2}(C_2^2-4)^{1/2}$, and the distribution resembles that of the one-photon laser. We note that the distribution is cylindrically symmetric, showing that all phases are equally probable.

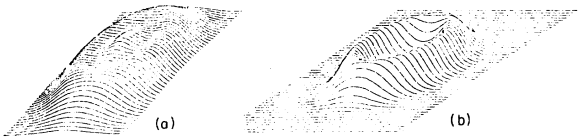

FIG. 8. Probability distribution for the two-photon laser (a) 1.1 × threshold; (b) 2 × threshold.

2. Photon statistics

The unnormalized intensity moments [cf. Eq. (3.5)] are

$$I^{(i)}=\int_0^\infty dR\left[1+\left(\frac{R}{n_0}\right)^2\right]^H e^{-R/\bar{n}}R^i dR=I^{(i)}(H). \tag{4.5}$$

Integration by parts yields a recursive relation for the moments which can then be expressed in terms of the zeroth moment which is

$$I^{(0)}(H)=\sqrt{\pi}\Gamma(H+1)\left(\frac{2}{z}\right)^{H+1/2}[H_{H+1/2}(z)-Y_{H+1/2}(z)], \tag{4.6}$$

where $z=n_0/\bar{n}$, $H_\nu(z)$ is a Struve function and Y_ν is a Bessel function. The mean photon number is then

$$\langle a^\dagger a\rangle=\frac{I^{(i)}}{I^{(0)}}=\frac{n_0^2\left(\frac{1}{\bar{n}}I^{(0)}(H+1)-1\right)}{2(H+1)I^{(0)}(H)}, \tag{4.7}$$

and the second-order correlation function $g^{(2)}(0)=\langle a^{\dagger 2}a^2\rangle/\langle a^\dagger a\rangle^2$ is

$$g^{(2)}(0)=\frac{(H+1)I^{(0)}(H)\left[\frac{1}{\bar{n}(H+2)}\left(\frac{1}{\bar{n}}I^{(0)}(H+2)-1\right)-\frac{2}{n_0^2}I^{(0)}(H+1)\right]}{\left(\frac{1}{\bar{n}}I^{(0)}(H+1)-1\right)^2}. \tag{4.8}$$

$\langle a^\dagger a\rangle$ and $g^{(2)}(0)$ are plotted in Fig. 7 as functions of the atomic pumping C_2, together with the semiclassical mean. For low noise (large z), $g^{(2)}(0)$ has the asymptotic values of 1 below threshold and 2 above threshold, similar to the one-photon laser. In contrast to the one-photon laser, however, there is a large enhancement of fluctuations in the threshold region, and $g^{(2)}(0)$ shows a pronounced maximum in this region. For more dominant noise this enhancement becomes less pronounced and the maximum in $g^{(2)}(0)$ shifts to lower C_2. In fact, for $z\simeq 1$, Fig. 7 shows there is practically no enhancement of fluctuations.

B. Two-photon laser with injected signal

Practical difficulties in realizing a two-photon laser arise from the low initial gain of the device. For small photon numbers the gain term is approximately $C_2|x|^2$ compared with C_1x for the one-photon case. The nonlinear coupling C_2 is generally much smaller than the coupling for the one-photon case, and $|x|^2$ is smaller than x when x is small. In order to enhance the initial gain then, an external signal may be injected.

1. Semiclassical theory

From Eq. (2.5), the state equation for the two-photon laser with an injected signal is

$$y = x\left(1 - \frac{C_2|x|^2}{1+|x|^4}\right). \tag{4.9}$$

Setting $y = y_0 e^{i\theta_0}$ and $x = re^{i\theta}$, we find

$$y_0 = -r\left(1 - \frac{C_2 r^2}{1+r^4}\right),$$

and

$$\theta = \begin{cases} \pi, & \text{for } 1 - \dfrac{C_2 r^2}{1+r^4} > 0 \\ \theta_0 + \pi, & \text{for } 1 - \dfrac{C_2 r^2}{1+r^4} < 0. \end{cases} \tag{4.10}$$

Figure 9 shows the state equation for various values of the pumping parameter. Below the lasing threshold $C_2 = 2$, the cavity field x is always in phase with the injected field y. For $C_2 \lesssim 1.14$, x is a monotonic function of y, but for $1.14 \lesssim C_2 < 2$, x is a triple-valued function over a certain range of y. The system thus exhibits bistability as a function of the injected driving field for $1.14 \lesssim C_2 < 2$. Above the lasing threshold $C_2 = 2$, x is a more complicated multiple valued function of y. The stability of the various branches in the multiple valued regions can be deduced from the stability conditions (2.8), which in this case have the same form as the stability equations (4.3) for the two-photon laser without injected signal. The unstable branches are indicated on the diagrams in Fig. 9.

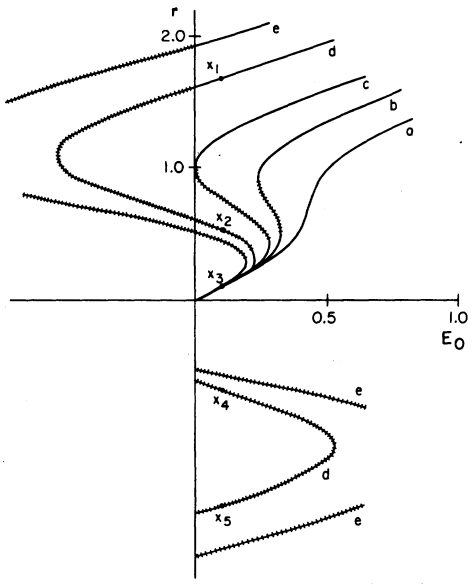

FIG. 9. Two-photon laser with an injected signal. Semiclassical amplitude r versus injected field amplitude E_0 for (a) $C_2 = 1$, (b) $C_2 = 1.5$, (c) $C_2 = 2$, (d) $C_2 = 3$, (e) $C_2 = 4$, //// unstable, —— stable.

2. Fluctuations

As with the other systems studied here, an examination of the potential gives perhaps a better understanding of the stability of the two-photon laser with an injected signal. The potential here is given by Eq. (2.14), with D_0 positive and $E \neq 0$. Converting to polar coordinate $\alpha = \sqrt{I}e^{i\theta}$ and $E = E_0 e^{i\theta_0}$, we have

$$\phi(I,\theta) = \frac{I}{\bar{n}} - \frac{2E_0}{\bar{n}}\sqrt{I}\cos(\theta - \theta_0) - H\ln\left(1 + \frac{I^2}{n_0^2}\right), \tag{4.11}$$

where $\bar{n}$ and H are as defined following Eq. (4.5). The turning points of the potential are the solutions of $\partial\phi/\partial r = 0 = \partial\phi/\partial\theta$ and correspond to the semiclassical solutions. The nature of these turning points is found by looking at the second derivatives of ϕ. Moving along the state equation curves for $C_2 > 2$ in Fig. 9, decreasing E_0, we find the following behavior: Points on the uppermost branch correspond to local minima in ϕ until $E_0 = 0$, where they become saddle points. Moving around and approaching E_0 from the negative side, points in this region become maxima, then again saddle points when $E_0 = 0$ is passed. At the next turning point the saddle point becomes a maximum, and the points on the curve from here on as $E_0 \to 0$ from the positive side correspond to maxima in ϕ. The negative r behavior follows from the odd symmetry. This behavior is shown in Fig. 10 where the probability distribution P is plotted. Since minima in ϕ correspond to maxima in P, it is readily apparent which of the turning points of ϕ correspond to stable steady states.

C. Two-photon optical bistability

As in the one-photon transition case, Eq. (2.4) can be used to describe the optical bistability which may occur when the passive atoms ($D_0 = -N/2$) in the cavity are excited via a two-photon transition.

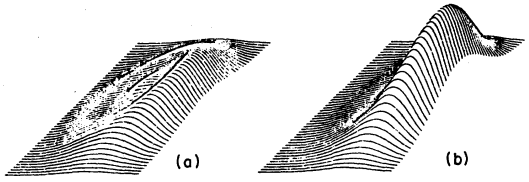

FIG. 10. Probability distribution for the two-photon laser with an injected signal 1.1 × threshold, $\theta_0 = 0$: (a) $E_0 = 0.25$, (b) $E_0 = 0.5$.

1. Semiclassical analysis

Taking $n=2$ for the two-photon transition, the state equation in the normalized variables $x=(4g^2/\gamma_\parallel\gamma_\perp)^{1/4}\alpha$ and $y=(4g^2/\gamma_\parallel\gamma_\perp)^{1/4}E$ is

$$y=x\left(1+\frac{C_2|x|^2}{1+|x|^4}\right), \tag{4.12}$$

where $C_2=-(2gD_0/\kappa)(\gamma_\parallel/\gamma_\perp)^{1/2}=(gN/\kappa)(\gamma_\parallel/\gamma_\perp)$. This equation describing two-photon optical bistability was first derived by Arecchi and Politi[30] and further theoretical work has been done by Agrawal and Flytzanis.[31] The effect has been recently observed experimentally by Grynberg *et al.*[32] A numerical analysis of Eq. (4.12) reveals that multiple value solutions only occur when C_2 exceeds the threshold value $C_2=5.42$.[30] The state equation is plotted in Fig. 11 for C_2 greater than this threshold value. The linearized stability analysis of Eq. (4.12) shows that the upper and lower branches are stable and the middle branch is unstable, so that in the multiple-value-solution region the system is bistable.

2. Fluctuations

When fluctuations are included, a Fokker-Planck equation of the form of (2.12) for the photon distribution can be derived. As with one-photon bistability, the Fokker-Planck equation only takes this form with a constant noise term $\bar{n}$ when the thermal noise $\bar{n}$ is much greater than the quantum noise. The steady-state solution for the probability distribution (Fig. 12) is given by Eqs. (2.13) and (2.14), with $n=2$ and $D_0=-N/2$:

$$\phi(r,\theta)=\frac{I}{\bar{n}}-2\frac{E_0}{\bar{n}}\sqrt{I}\cos(\theta-\theta_0)+\frac{\gamma_\parallel N}{\Lambda}\ln\left[1+\left(\frac{I}{n_0}\right)^2\right], \tag{4.13}$$

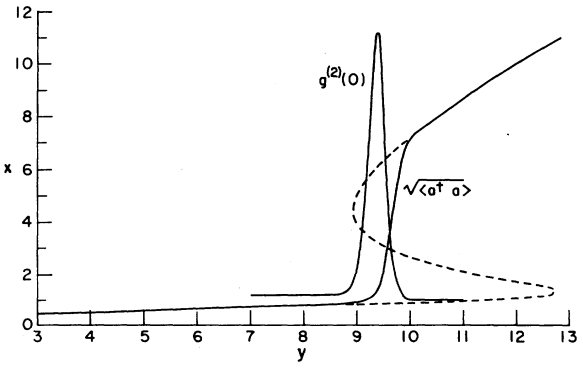

FIG. 11. Moments for two-photon bistability. Root-mean-square intensity $(\langle a^\dagger a\rangle)^{1/2}$ and second-order correlation function $g^{(2)}(0)$ versus driving field amplitude y; semiclassical root-mean intensity ---. Parameters $C_2=20$, $n_0=1$, $\bar{n}=1$.

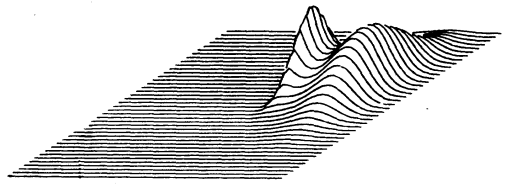

FIG. 12. Probability distribution for two-photon bistability.

where we have used the polar coordinates $\alpha=\sqrt{I}e^{i\theta}$ and $E=E_0e^{i\theta_0}$. The nonnormalized moments of this distribution are

$$I^{(i)}=\int d^2\alpha\,|\alpha|^{2i}P(\alpha,\alpha^*)=\sum_{k=0}^{\infty}\frac{(E_0/\bar{n})^{2k}}{(k!)^2}\int_0^\infty dR\left[1+\left(\frac{R}{n_0}\right)^2\right]^{-H}R^{i+k}e^{-R/\bar{n}}. \tag{4.14}$$

In each case the integrals were evaluated numerically. The mean $\langle a^\dagger a\rangle=I^{(1)}/I^{(0)}$ is plotted in Fig. 11 together with the semiclassical mean for comparison. Also plotted in Fig. 11 is the second-order correlation function $g^{(2)}(0)$. The qualitative behavior is the same as for the one-photon case (Fig. 5). An important quantitative difference is that in the two-photon case fluctuations on the lower branch are less than in the one-photon case. In the one-photon case $g^{(2)}(0)$ tends to the thermal value of 2 whereas in the two-photon case $g^{(2)}(0)$ is closer to 1. This is to be expected because the two-photon absorption removes pairs of photons[33] thus decreasing $g^{(2)}(0)$, which is a measure of the coincident pairs of photons. However, in our analysis the fluctuations on the upper branch cannot be reduced below the $g^{(2)}(0)=1$ of the one-photon case. The nonclassical region $g^{(2)}(0)<1$ requires a nonpositive definite noise matrix in the Fokker-Planck equation, which is not possible when only thermal noise is considered.

D. Two-photon saturable absorber with chaotic driving field

In this section we look at the two-photon version of the saturable absorber driven by a completely chaotic field. In this case E is zero, and the noise term $\bar{n}$ is proportional to the intensity of the input chaotic field. The passive atoms in the cavity are now assumed to be excited via a two-photon transition. We can use the analysis of the preceding section by setting the coherent input E equal to zero. From Eq. (4.13), the steady-state P function is thus

$$P(\alpha,\alpha^*)=N\left[1+\left(\frac{|\alpha|^2}{n_0}\right)^2\right]^{-H}e^{-|\alpha|^2/\bar{n}}. \tag{4.15}$$

The nonnormalized intensity moments are then given by Eq. (4.14), with $E_0=0$:

$$I^{(l)}=\int_0^\infty dR\left[1+\left(\frac{R}{n_0}\right)^2\right]^{-H}e^{-R/\bar{n}}R^l. \tag{4.16}$$

To obtain the moments used here, these integrals were computed numerically. In Fig. 13(a), the second-order correlation function $g^{(2)}(0)$ is plotted as a function of the normalized intensity $2\Lambda/\gamma_{\parallel}D_0$ of the chaotic driving field for various values of the cooperativity parameter C_2. These particular normalized variables were chosen in order to make comparison with the one-photon results of Ref. 4. The two-photon results are qualitatively similar to those of the one-photon case. Although there is no bistability in the output intensity, there is still a "threshold" region centered around $2\Lambda/\gamma_{\parallel}D_0=1$, where the cavity-field fluctuations are enhanced far above the thermal value $g^{(2)}(0)=2$. This occurs when the atoms begin saturating. This region is followed by the "saturation" region, where the input field is strong enough to saturate the atoms and the input field passes straight through without appreciable interaction with the atoms. $g^{(2)}(0)$ thus drops to the value of 2, corresponding to the chaotic input field. The main difference from the one-photon case is the behavior for the low driving intensities of the pretransition region, where the atoms are linear, showing virtually no saturation effects at all. In the one-photon case this linear interaction does not change the statistics of the field and thus $g^{(2)}(0)\simeq 2$, the value for the chaotic input field. However, in the two-photon case, the interaction

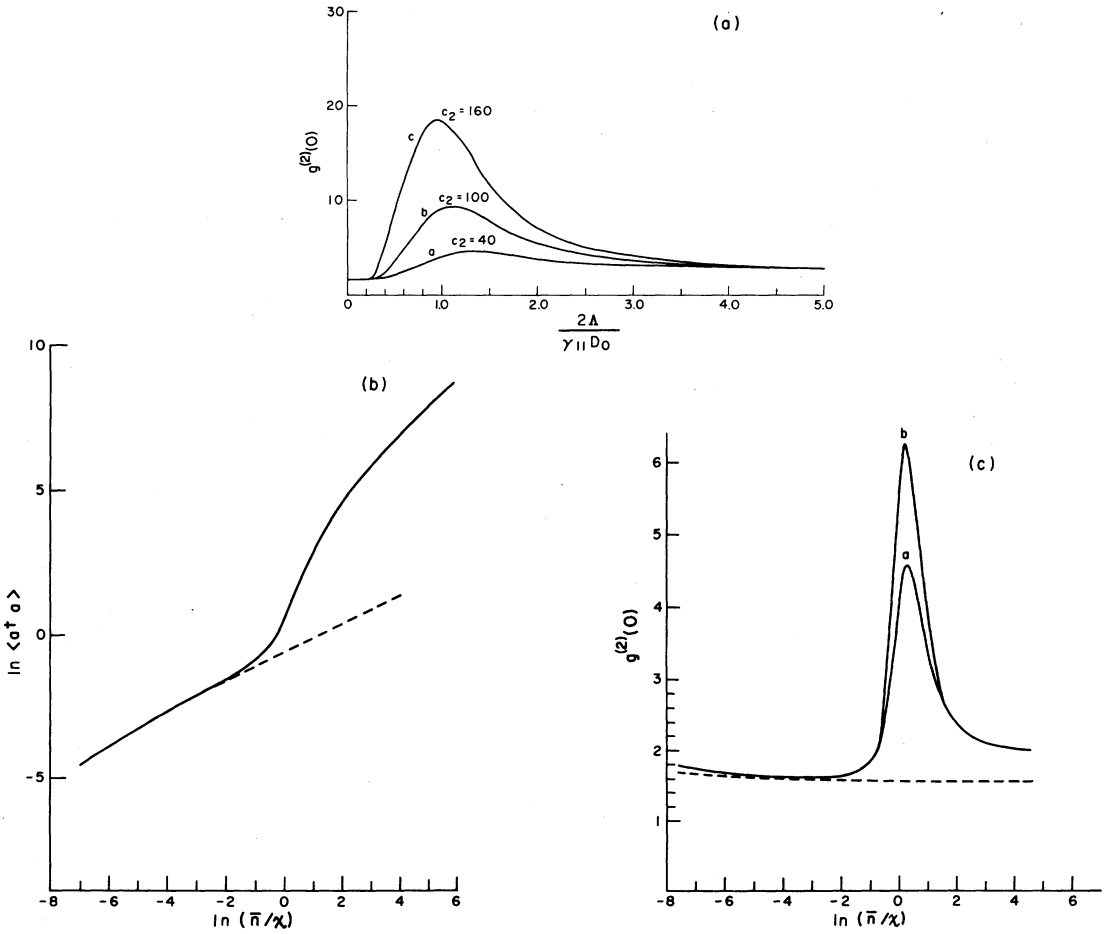

FIG 13. (a) Two-photon saturable absorber with chaotic driving field. Second-order correlation function $g^{(2)}(0)$ versus normalized driving-field intensity $2\Lambda/\gamma_{\parallel}D_0$. Curve a $C_2=40$, curve b $C_2=100$, and curve c $C_2=160$. (b) Two-photon absorber with chaotic driving field. $\ln\langle a^\dagger a\rangle$ vs $\ln(\bar{n}/\chi)$ for nonsaturable (----) and saturable (——) absorber; $C_2=40$ and $n_0=1$. (c) Two-photon absorber with chaotic driving field. Second-order correlation function $g^{(2)}(0)$ vs $\ln(\bar{n}/\chi)$ for nonsaturable (----) and saturable (——) absorber; curve a, $C_2=40$, and curve b, $C_2=80$, $n_0=1$.

with the atoms removes photons in pairs, so $g^{(2)}(0)$ is less than the chaotic value of 2.

The behavior of a two-photon saturable absorber with a mixed coherent and Gaussian driving field is described by the same equations as for two-photon optical bistability, in Sec. IV C. In this case, the amplitude of the coherent part of the field is given by E_0, and the intensity of the Gaussian component is given by $\bar{n}$. Thus, Fig. 11, which shows the intensity and $g^{(2)}(0)$ for optical bistability, also corresponds with the two-photon saturable absorber with mixed driving field. However, in Fig. 11, the parameter values are such that the thermal, or Gaussian component is too small to cause any appreciable saturation when the coherent component E is zero. As the thermal component is increased, however, the atoms begin saturating, and the rise in $g^{(2)}(0)$ occurs at lower values of the coherent field. If the thermal component is so large that saturation effects are significant even when the coherent field E_0 is zero, $g^{(2)}(0)$ is already large at $E_0=0$ and shows no further increase when E_0 is increased. In this situation the mean photon number does not follow the lower branch of the semiclassical-state equation to any good approximation.

1. Nonsaturating two-photon absorber

It is of interest to compare the above results with those for a two-photon absorber with no saturation effects. A Hamiltonian describing such an absorber is[34]

$$H=\Gamma_2 a^{\dagger 2}+\Gamma_2^{\dagger} a^2+\Gamma_F a^{\dagger}+\Gamma_F^{\dagger} a + i\hbar(a^{\dagger}\epsilon e^{-i\omega_0 t}-a\epsilon^* e^{i\omega_0 t}) . \tag{4.17}$$

As in Sec. II, Γ_F and $\Gamma_F^{\dagger}$ are reservoir operators for the damping of the field and ϵ is proportional to the coherent part of the driving field, which has frequency ω_0. The two-photon interaction now occurs via a reservoir of atoms, described by the reservoir operators Γ_2 and $\Gamma_2^{\dagger}$. Since the field interacts with a reservoir of atoms, saturation does not occur. Using standard techniques,[35] the two reservoirs may be eliminated to get the following Fokker-Planck equation for the field quasiprobability distribution:

$$\frac{\partial P(\alpha,\alpha^*)}{\partial \tau}=\left(-\frac{\partial}{\partial \alpha}[-(\alpha-E)-2\chi|\alpha|^2\alpha] - \frac{\partial}{\partial \alpha^*}[(\alpha^*-E^*)-2\chi|\alpha|^2\alpha^*] + 2\bar{n}\frac{\partial^2}{\partial\alpha\partial\alpha^*}\right)P(\alpha,\alpha^*), \tag{4.18}$$

where χ is proportional to the two-photon absorption rate, $\tau=kt$, and $kE=\mathcal{E}$. We have assumed the thermal noise is dominant and have neglected quantum noise terms which may be included using a generalized P representation.[36] The steady-state solution for the P function when $E=0$ is

$$P(\alpha)=N\exp\left(-\frac{1}{\bar{n}}(|\alpha|^2+\chi|\alpha|^4)\right); \tag{4.19}$$

the nonnormalized moments of the distribution are

$$I^{(i)}=\int_0^{\infty} dR\, R^i e^{-(1/\bar{n})(R+\chi R^2)} . \tag{4.20}$$

$\ln\langle a^{\dagger}a\rangle$ and $g^{(2)}(0)$ for the nonsaturable absorber are plotted in Figs. 13(b) and 13(c) for comparison with the saturable absorber result. As expected, both give the same result for small values of the incoherent driving intensity $\bar{n}$. Since the reservoir never saturates, $g^{(2)}(0)$ for the nonsaturable absorber shows no peak, unlike the saturable absorber. In the saturable case, once the atoms have saturated, the cavity field is just the chaotic driving field which no longer interacts with the atoms and $g^{(2)}(0)$ thus tends to two for large $\bar{n}$. In the nonsaturable case, the reservoir atoms continue to absorb even for large $\bar{n}$, giving a nonthermal value $g^{(2)}(0)<2$. We note that the P function [Eq. (4.19)] is, in fact, a limiting case of the result derived in Sec. II [Eqs. (2.13) and (2.14)]. If the log term in Eq. (2.14) is expanded and only the first term in the expansion retained, we obtain Eq. (4.19) with the identification $\chi=2C$. Thus, as expected, the saturable absorber follows the behavior of the nonsaturable absorber for small field intensities $|\alpha|^2 \ll n_0$.

V. DISCUSSION

We have given a unified description of light which interacts resonantly with atoms in a cavity via an n-photon transition. In the good (high-Q) cavity limit a single equation describes the light field in an n-photon laser, and n-photon laser with an injected signal or n-photon optical bistability, depending on the values of the parameters representing the external driving field and external incoherent pumping of the atoms.

In the limit where quantum noise can be neglected in comparison with thermal noise, fluctuations may be taken into account simply, and a single general Fokker-Planck equation governing the statistical distribution of the light is derived. The steady-state solution of this equation is readily obtained, giving a general expression from which any statistical properties for any situation can be calculated. Although only thermal noise is taken into account, this still allows considera-

tion of effects due to noise from spontaneous emission by the atoms or any chaotic component (Gaussian fluctuations) superimposed on the coherent driving field; it even allows analysis of situations where the driving field is completely chaotic, with no coherent part at all.

Explicit calculations of semiclassical and statistical properties were done for the one-photon and two-photon transition cases. In the one-photon laser case, the distribution retained the saturation term accounted for only approximately in earlier works. However, the recent work by Mandel[43] is even more accurate in that it also includes some quantum noise, as well as the saturation term. For one-photon optical bistability the second-order correlation function $g^{(2)}(0)$ was calculated using the fully two-dimensional distribution, that is, retaining both amplitude and phase. While no different qualitatively from previous works in which the phase was ignored, it was nevertheless a more accurate expression.

Previous work on the photon statistics of the two-photon laser has concentrated on the Scully and Lamb[12] birth-death-type master equation approach. Here we have approached the problem using a Fokker-Planck equation and its corresponding potential. This approach is particularly useful for comparison with the semiclassical behavior, and making analogies between this nonequilibrium steady-state behavior and the phase transitions of equilibrium statistical mechanics.

Our analysis of two-photon optical bistability includes for the first time an analysis of the photon statistics of the output light field; previous workers have considered only the deterministic aspects of the problem. Here we have shown that, with a few obvious differences due to the two-photon atomic transition, in the thermal noise limit the two-photon optical bistability behavior is qualitatively similar to that of the one-photon situation. It should be noted that when the atomic transition is a multiphoton one, there arise intensity dependent Stark shift terms.[30,31] In general, these are small and can be ignored, but if necessary they can be readily included in our analysis. The final problem considered in this work is the two-photon saturable absorber driven by a completely chaotic input, the same system that exhibits two-photon optical bistability when driven by a coherent input. This is a problem which up until now has received no attention in the literature. Again, apart from expected differences, the behavior is similar to that in the one-photon case, with a strong enhancement of the second-order correlation function in the saturating region even though the bistable behavior no longer exists.

As a final comment we note that in the multiple-steady-state situations, it is straightforward to calculate various macroscopic transition times analogously to the one-photon cases. When fluctuations are considered, the stable multiple steady states determined by the semiclassical equations become metastable; internal fluctuations can cause the systems to shift from one steady state to another, even though the external conditions are unchanged. The time for such changes to occur, the tunneling time, can be calculated using the method derived by Kramers,[37] as done, for example, for one-photon optical bistability in Ref. 23. Another time of interest, especially when considering such systems as switching devices, is the switching time. This is the time taken, for example, by a system which exhibits bistability to attain its new steady state when the driving field is suddenly changed so that the corresponding steady state changes from the lower to the upper branch or vice versa. This time may be estimated by solving the semiclassical equations of motion to obtain the full time dependence of the output field, as done for sub/second harmonic generation[38] and one-photon optical bistability.[39]

---

*Visitor at JILA, on leave from the Physics Department, University of Waikato, Hamilton, New Zealand.

[1]R. Graham and A. Schenzle, Phys. Rev. A 23, 1302 (1981).
[2]H. Haken, Handb. Physik. 25/2c (Springer, Berlin, 1970).
[3]M. Lax, in *Brandeis University Summer Institute Lectures*, Vol. 11, edited by M. Chretien, E. P. Gross, and S. Desev (Gordon and Breach, New York, 1966).
[4]P. Mandel, Phys. Rev. A 21, 2020 (1980).
[5]H. Risken, Z. Phys. 186, 85 (1965).
[6]L. Lugiato, Nuovo Cimento 50B, 89 (1979).
[7]P. D. Drummond and D. F. Walls, Phys. Rev. A 23, 2563 (1981).
[8]H. Haken, Rev. Mod. Phys. 47, 67 (1975).
[9]W. E. Lamb, Jr., Phys. Rev. 134, A1429 (1964).
[10]V. Degiorgio and M. O. Scully, Phys. Rev. A 2, 1170 (1970).
[11]R. Graham and H. Haken, Z. Phys. 237, 31 (1970).
[12]*Handbook of Mathematical Functions*, edited by M. Abramowitz and I. A. Stegun (Dover, New York, 1965).
[13]M. O. Scully and W. E. Lamb, Jr., Phys. Rev. 159, 208 (1967).
[14]M. Lax and W. Louisell, IEEE J. Quantum Electron. 3, 47 (1967).

[15]F. T. Arecchi, V. Degiorgio, and B. Querzola, Phys. Rev. Lett. 19, 1168 (1967).
[16]L. Lugiato, Lett. Nuovo Cimento 23, 609 (1978).
[17]P. D. Drummond, Ph.D. thesis, University of Waikato, 1979 (unpublished).
[18]W. W. Chow, M. O. Scully, and E. W. van Stryland, Opt. Commun. 15, 6 (1975).
[19]R. Bonifacio and L. Lugiato, Opt. Commun. 19, 172 (1976).
[20]W. J. Sandle, in *Proceedings of the Second New Zealand Summer School in Laser Physics*, edited by D. F. Walls and J. D. Harvey (Academic, New York, 1980).
[21]R. Bonifacio, M. Gronchi, and L. A. Lugiato, Phys. Rev. A 18, 2266 (1978).
[22]A. Schenzle and H. Brand, Opt. Commun. 27, 485 (1978).
[23]P. D. Drummond, K. J. McNeil, and D. F. Walls, Phys. Rev. A 22, 1672 (1980).
[24]K. J. McNeil and D. F. Walls, J. Phys. A 8, 104 (1975).
[25]R. Görtz and D. F. Walls, Z. Phys. 25B, 423 (1976).
[26]H. Ito and T. Nakagomi, Prog. Theor. Phys. 57, 54 (1977).
[27]A. R. Bulsara and W. C. Schieve, Phys. Rev. A 19, 2046 (1979).
[28]N. Nayak and B. K. Mohanty, Phys. Rev. A 19, 1204 (1979).
[29]L. Sczaniecki, Opt. Acta 27, 251 (1980).
[30]F. T. Arecchi and A. Politi, Lett. Nuovo Cimento 23, 65 (1978).
[31]G. P. Agrawal and C. Flytzanis, Phys. Rev. Lett. 44, 1058 (1980).
[32]G. Grynberg, E. Giacobino, M. Devaud, and F. Biraben, Phys. Rev. Lett. 45, 434 (1980).
[33]P. Lambropoulos, Phys. Rev. 156, 286 (1967).
[34]S. Chaturvedi, P. D. Drummond, and D. F. Walls, J. Phys. A 10, L187 (1977).
[35]W. Louisell, *Quantum Statistical Properties of Radiation* (Wiley, New York, 1973).
[36]P. D. Drummond and C. W. Gardiner, J. Phys. A 13, 2353 (1980).
[37]H. A. Kramers, Physica (Utrecht) 7, 284 (1940).
[38]P. D. Drummond, K. J. McNeil, and D. F. Walls, Opt. Acta 27, 321 (1980).
[39]V. Benza and L. A. Lugiato, Lett. Nuovo Cimento 26, 405 (1979).